

Diffuse PeV neutrinos from gamma-ray bursts

Ruo-Yu Liu^{1,2,3} and Xiang-Yu Wang^{1,4}

ABSTRACT

The IceCube collaboration recently reported the potential detection of two cascade neutrino events in the energy range 1-10 PeV. We study the possibility that these PeV neutrinos are produced by gamma-ray bursts (GRBs), paying special attention to the contribution by untriggered GRBs that elude detection due to their low photon flux. Based on the luminosity function, rate distribution with redshift and spectral properties of GRBs, we generate, using Monte-Carlo simulation, a GRB sample that reproduce the observed fluence distribution of Fermi/GBM GRBs and an accompanying sample of untriggered GRBs simultaneously. The neutrino flux of every individual GRBs is calculated in the standard internal shock scenario, so that the accumulative flux of the whole samples can be obtained. We find that the neutrino flux in PeV energies produced by untriggered GRBs is about 2 times higher than that produced by the triggered ones. Considering the existing IceCube limit on the neutrino flux of triggered GRBs, we find that the total flux of triggered and untriggered GRBs can reach at most a level of $\sim 10^{-9} \text{ GeV cm}^{-2} \text{ s}^{-1} \text{ sr}^{-1}$, which is insufficient to account for the reported two PeV neutrinos. Possible contributions to diffuse neutrinos by low-luminosity GRBs and the earliest population of GRBs are also discussed.

Subject headings: diffuse background : neutrinos — gamma rays: bursts

1. Introduction

Detection of high-energy neutrinos would be an important step towards identifying the origin of cosmic rays. Interestingly, through analysis designed to search for ultra high-energy ($\gtrsim \text{PeV}$) and high quality shower events over a period of 672.7 live days between 2010 and 2012 with IceCube, two PeV neutrino-induced cascade events have been found (Ishihara 2012). The two events were observed on August 9, 2011 and January 3, 2012, and each have an energy of approximately 1-10

¹School of Astronomy and Space Science, Nanjing University, Nanjing, 210093, China

²Max-Planck-Institut für Kernphysik, 69117 Heidelberg, Germany

³Fellow of the International Max Planck Research School for Astronomy and Cosmic Physics at the University of Heidelberg (IMPRS-HD)

⁴Key laboratory of Modern Astronomy and Astrophysics (Nanjing University), Ministry of Education, Nanjing 210093, China

PeV. The observation of two events with an expected background of 0.14 events from the atmospheric neutrinos corresponds to a significance of 2.36σ . Given this modest statistical significance, we cannot at this time be confident that they are of astrophysical origin.

Gamma-ray bursts (GRBs) have been proposed as a potential source of ultra-high energy cosmic rays (UHECRs) (e.g. Waxman 1995; Vietri 1995; Dermer 2002), and high energy neutrino emission has been predicted to be produced in the dissipative fireballs, where cosmic ray protons interact with fireball photons (e.g. Waxman & Bahcall 1997; Dermer & Atoyan 2006; Guetta et al. 2004; Murase et al. 2006; Wang & Dai 2009). Gamma-ray bursts are an attractive possibility for the reported two PeV neutrinos because the predicted neutrino emission in the standard internal shock model peaks at PeV energies. Notably, previous searches of GRB neutrinos with IceCube via stacking analysis of many triggered GRBs have yield none detection (Abbasi et al. 2010, 2011, 2012). The approach to search for neutrinos from triggered GRBs is through analysis of upgoing neutrinos that are correlated in time and direction with known GRBs, which is different from that of detecting diffuse neutrinos. The most stringent constraint is given by the combined analysis of the IceCube 40- and 59-string (IC40+59) data of upgoing neutrinos from 215 triggered GRBs, which leads to an upper limit that is claimed to be below the expected flux (Abbasi et al. 2012)¹. Beside the contribution by triggered GRBs for which the stacking analysis has been performed, GRBs that do not trigger detectors due to their low flux may also contribute to the diffuse neutrino flux. The purpose of this paper is to study whether the sum contribution of triggered GRBs and untriggered GRBs can explain the reported two PeV neutrinos under the constraint that the stacked neutrino flux of 215 triggered GRBs is below the IC40+59 sensitivity. The untriggered GRBs defined in our paper are normal GRBs (i.e. belonging to the normal GRB population) that do not trigger the current detectors. They are normal GRBs in the low-luminosity end of the luminosity function (for normal GRBs) and/or locating at high redshifts and hence they can elude the detection by current GRB detectors (e.g. Fermi/GBM) due to the limited sensitivity.

Previous estimates of diffuse neutrino flux from GRBs are made through integrating the neutrino flux over the whole luminosity range and the redshift range of GRBs, assuming that the their number density follows a given luminosity function and redshift distribution function (e.g. Gupta & Zhang 2007; He et al. 2012; Cholis & Hooper 2012). The estimates show that the total flux from all the GRBs (including both the triggered ones and the untriggered ones) reach a level of $\sim 10^{-9} - 10^{-8} \text{GeVcm}^{-2}\text{s}^{-1}\text{sr}^{-1}$ (Gupta & Zhang 2007; He et al. 2012; Cholis & Hooper 2012), which depends on the luminosity function and redshift distribution that are used. These estimates made simplified assumptions about some properties of GRBs, e.g. assuming the same photon spectrum for every GRBs, and do not consider the existing IceCube limit on triggered GRBs. To overcome this simplification, we here present a new approach to calculate the diffuse neutrino flux.

¹This claim is based on the theoretic flux obtained with the formula in Guetta et al. (2004). Recent calculations show, however, that the previous calculation may overestimate the flux of GRB neutrinos (Li 2012; Hümmer et al. 2012; He et al. 2012).

We generate a GRB sample with Monte-Carlo simulation², requiring that the triggered population of GRBs reproduce the observed properties of Fermi/GBM GRBs. A population of dim, untriggered GRBs will be generated simultaneously in the simulation. Then, the neutrino flux of every individual GRBs are calculated, so that the accumulative flux of the whole sample can be obtained.

The rest part of this paper is arranged as follows. In §2, we describe the properties of GRBs and some empirical relations used in our simulation generating the GRB sample. We calculate the accumulative neutrino flux from both triggered GRBs and untriggered GRBs in the generated sample and compare them with the reported two PeV events in §3. We give our discussion and conclusion in §4 and 5. Throughout the paper, we use eV for particle energy, c.g.s units for other quantities and denote by Q_x the value of the quantity Q in units of 10^x unless specified.

2. Simulation of a GRB sample

The distributions of GRBs in luminosity and in redshift are assumed to be independent of each other in this work, i.e., $n(L, z) = \phi(L)\rho(z)$, where $\phi(L)$ and $\rho(z)$ are luminosity function and redshift distribution function of GRBs respectively. Wanderman & Piran (2010, hereafter, W10) obtained the luminosity function and cosmic rate by inverting directly the redshift - luminosity distribution of observed long Swift GRBs, which are, respectively, given by

$$\phi(L) = \begin{cases} \left(\frac{L}{L_*}\right)^{-a_1}, & L < L_* \\ \left(\frac{L}{L_*}\right)^{-a_2}, & L \geq L_* \end{cases} \quad (1)$$

and

$$\rho(z) = \rho_0 \text{Gpc}^{-3} \text{yr}^{-1} \begin{cases} (1+z)^{n_1}, & z < z_* \\ (1+z)^{n_2} (1+z_*)^{n_1-n_2}, & z \geq z_* \end{cases} \quad (2)$$

where $a_1 = 1.2$, $a_2 = 2.4$, $L_* = 10^{52.5} \text{ergs}^{-1}$, $n_1 = 2.1$, $n_2 = -1.4$, $z_* = 3.1$, and $\rho_0 = 1.3 \text{Gpc}^{-3} \text{yr}^{-1}$ are the best fit parameters. Note that L is the isotropic, peak bolometric luminosity of GRBs in energy range 1 keV–10 MeV. The low- and high- luminosity ends of the luminosity function are set as 10^{50}ergs^{-1} and 10^{54}ergs^{-1} respectively, and the maximum redshift is set as $z_{\text{max}} = 8$. We generate a sample of GRBs that follow the luminosity distribution and redshift distribution given by Eq. 1 and Eq. 2 with Monte-Carlo simulation. The isotropic energy of each GRBs is obtained through the relation

$$\log E_{\text{iso},52} = 1.07 \log L_{\text{iso},52} + (0.66 \pm 0.54) \quad (3)$$

which is obtained from the data in Ghirlanda et al. (2012). The photon spectra of GRBs can be described by an empirical function known as the Band function (Band et al. 1993), which can be

² A similar approach of sampling the bursts individually using a Monte-Carlo algorithm was made by Baerwald et al. (2012) to obtain a more complete sample of GRBs.

written as

$$N(E) = N_0 \begin{cases} \left(\frac{E}{E_0}\right)^\alpha e^{-E/E_0}, & E < (\alpha - \beta)E_0 \\ \left(\frac{E}{E_0}\right)^\beta (\alpha - \beta)^{\alpha-\beta} e^{\beta-\alpha}, & E \geq (\alpha - \beta)E_0 \end{cases} \quad (4)$$

where N_0 is the normalization constant and α, β are the photon indices for low- and high-energy spectra respectively. Generally, $\alpha > -2$ and $\beta < -2$, and the energy spectrum peaks at $E_{\text{peak}} = (2 + \alpha)E_0$. The values of α and β are generated following the observed distribution of BATSE long GRBs in the simulation and only bursts with $\beta < -2$ are adopted (Kaneko et al. 2006). The rest frame peak energy of GRBs is found to be correlated with their isotropic energy and luminosity, which are known as the Amati relation and the Yonetoku relation, respectively (Amati et al. 2002; Yonetoku et al. 2004). In this work, to generate the peak energies of GRBs in the simulation, we adopt the $E_{\text{peak}} - E_{\text{iso}}$ relation recently found by Ghirlanda et al. (2012), i.e.

$$\begin{aligned} \log \left(\frac{E_{\text{peak}}}{\text{keV}} \right) &= \log \left(\frac{E_{\text{peak}}^{\text{ob}}(1+z)}{\text{keV}} \right) \\ &= 0.56 \log \left(\frac{E_{\text{iso}}}{\text{erg}} \right) - 26.06 \pm 1.14, \end{aligned} \quad (5)$$

where $E_{\text{peak}}^{\text{ob}}$ is the observer frame peak energy (hereafter the subscript "ob" represents the quantity in the observer frame). Since the neutrino emission is produced dominantly by long duration GRBs, we only include bursts with $T_{90} > 2\text{s}$ in our sample. Following Kakuwa et al. (2012), we determine T_{90} roughly by $T_{90} = (1+z)(E_{\text{iso}}/L_{\text{ave}})$ where $L_{\text{ave}} = 0.3L_{\text{iso}}$ is the average luminosity of a GRB.

To compare our simulated sample with observed GRBs by *Fermi*/GBM, the trigger threshold in our simulation is set to be the same as that of *Fermi*/GBM, i.e., $0.74 \text{ photons cm}^{-2} \text{ s}^{-1}$ (Meegan et al. 2009). Taking into account the effect of Earth occultations and the South Atlantic Anomaly (SAA) passages, about 65% GRBs above the *Fermi*/GBM trigger threshold can be observed. To reproduce the GBM detection rate of ~ 250 GRBs per year, the value of ρ_0 is required to be $1.01 \text{ Gpc}^{-3} \text{ yr}^{-1}$, which is within the 1σ error of the best-fit value obtained by W10. For this value of ρ_0 , the total event rate of GRBs in the luminosity range from $10^{50} \text{ ergs}^{-1}$ to $10^{54} \text{ ergs}^{-1}$ and redshift range from $z = 0$ to $z = 8$ is ~ 8000 GRBs per year in the generated sample so the vast majority of them are untriggered GRBs. The total number of GRBs occurred from $z = 0$ to $z = 8$ per year is obtained through $N = \int 4\pi D_c^2(z) \frac{\rho(z)}{1+z} dD_c$, where $D_c(z) = \int_0^z \frac{cdz}{H(z)}$ with $H(z) = H_0 \sqrt{(1+z)^3 \Omega_M + \Omega_\Lambda}$ being the Hubble constant at redshift z in a flat universe.

In Fig. 1, we compare the 10–1000keV fluence distributions $dP/d(\log F_\gamma)$ of GRBs above the trigger threshold in our simulated sample with that of 482 *Fermi*/GBM bursts³. The K-S test of two distributions returns a high accepting probability of 89.5%. The total gamma-ray fluence of GRBs in 10–1000keV above the trigger threshold in our simulated sample is $0.0048 \text{ erg cm}^{-2}$ when

³From GRB 080714A to GRB 100704, data are taken from <http://heasarc.gsfc.nasa.gov/W3Browse/all/fermigbrst.html>

the number of bursts is normalized to be 482, which also agree well with the total gamma-ray fluence, $0.0044 \text{ erg cm}^{-2}$, of the observed 482 GBM bursts.

In Fig. 2 we show the distribution of the cumulative bolometric fluence $\sum_i F_{\gamma,i}(> F_{\gamma,th})$ above a certain flux $F_{\gamma,th}$ for the subsample of both triggered and untriggered GRBs. As is shown, the total gamma ray fluence of the untriggered GRBs ($F_{\gamma,unt} = 0.0136 \text{ erg cm}^{-2}$) is 2-3 times larger than that of the triggered ones ($F_{\gamma,tri} = 0.0053 \text{ erg cm}^{-2}$). This is mainly due to two aspects. First, the number of untriggered GRBs is much larger than that of triggered GRBs, although the luminosity of untriggered GRBs is on average much lower than that of triggered GRBs; Second, a fraction (about 35%) of bright GRBs occulted by the Earth also contribute to the gamma-ray fluence in the untriggered GRBs. This demonstrates that the total contribution of untriggered GRBs can be important.

There is significant variation in the luminosity function and the redshift distribution of GRBs in the literature, see e. g. Liang et al. (2007, hereafter, L07)⁴ and Guetta & Piran (2007, hereafter, G07)⁵. We find that the GRB sample generated using the above approach with the luminosity function and rate redshift distribution given in L07 contain much more triggered GRBs than the observed ones, while the G07 luminosity function in combination with the relevant redshift distribution gives rise to too few triggered GRBs. In other words, to maintain the rate of triggered GRBs of 250/yr by Fermi/GBM, ρ_0 is required to be $\sim 0.2 \text{ Gpc}^{-3} \text{ yr}^{-1}$ and $\sim 5 \text{ Gpc}^{-3} \text{ yr}^{-1}$ for L07 and G07 respectively, which are beyond the 3σ error of the best-fit values ($1.12 \text{ Gpc}^{-3} \text{ yr}^{-1}$ and $0.27 \text{ Gpc}^{-3} \text{ yr}^{-1}$ for L07 and G07 correspondingly). So here we adopt the luminosity function and redshift distribution of W10 in generating the GRB sample in our simulation.

⁴The luminosity function obtained by L07 is

$$\frac{dN}{dL_\gamma} = \rho_0 \Phi_0 \left[\left(\frac{L_\gamma}{L_{\gamma b}} \right)^{\alpha_1} + \left(\frac{L_\gamma}{L_{\gamma b}} \right)^{\alpha_2} \right]^{-1}, \quad (6)$$

where $\rho_0 = 1.12 \text{ Gpc}^{-3} \text{ yr}^{-1}$ is the local rate of GRBs, and Φ_0 is a normalization constant to assure the integral over the luminosity function being equal to the local rate ρ_0 . This luminosity function breaks at $L_{\gamma b} = 2.25 \times 10^{52} \text{ erg s}^{-1}$, with indices $\alpha_1 = 0.65$ and $\alpha_2 = 2.3$ below and above the break. The rate distribution with redshift used by L07 in obtaining this luminosity function is $S(z) = 23e^{3.4z} / (e^{3.4z} + 22.0)$ (Porciani & Madau 2001).

⁵The luminosity function obtained by G07 has the same form as that of W10, but has different parameter values, i.e., $\rho_0 = 0.27 \text{ Gpc}^{-3} \text{ yr}^{-1}$, $a_1 = -1.1$, $a_2 = -3.0$ and $L_* = 2.3 \times 10^{51} \text{ erg s}^{-1}$. This luminosity function is obtained based on the assumption that the rate of GRBs follows the star formation history given by Rowan-Robinson (1999), i.e.

$$S(z) = \begin{cases} 10^{0.75z} & z < 1, \\ 10^{0.75} & z \geq 1. \end{cases} \quad (7)$$

3. Diffuse neutrino emission from our GRB sample

3.1. Analytical calculation of neutrino flux

To illustrate the dependence of neutrino flux on the parameters, we first present an analytical approximation of calculating the neutrino flux.

It has been suggested that protons can be accelerated up to $\epsilon_p^{\text{ob}} \sim 10^{20} \text{eV}$ through internal or external shocks (e.g. Waxman 1995; Vietri 1995; Wang et al. 2008; Murase et al. 2008). The accelerated protons collide with the fireball photons in the same region and produce charged pions. The charged pions decay into four final-state leptons via the processes $\pi^+(\pi^-) \rightarrow \nu_\mu(\bar{\nu}_\mu) + \mu^+(\mu^-) \rightarrow \nu_\mu(\bar{\nu}_\mu) + e^+(e^-) + \nu_e(\bar{\nu}_e) + \bar{\nu}_\mu(\nu_\mu)$. In the fireball comoving frame, the fractional energy loss rate of a proton with Lorentz factor γ_p via photopion production is

$$t_{p\gamma}^{-1} = \frac{c}{2\gamma_p^2} \int_{\tilde{E}_0}^{\infty} d\tilde{E} \sigma_\pi(\tilde{E}) \xi(\tilde{E}) \tilde{E} \int_{\tilde{E}/2\gamma_p}^{\infty} dx x^{-2} n(x), \quad (8)$$

where c is the speed of light, \tilde{E} is the photon energy in the rest frame of the proton and \tilde{E}_0 is the threshold energy of photopion production. σ_π is the cross section of photopion production and ξ is the inelasticity. x and $n(x)$ are the photon energy and the photon spectrum in the GRB comoving frame respectively. When only the Δ resonance channel for the photopion production is considered, the fraction of the proton energy converted into the pion can be approximated by

$$f_{p\gamma}(\epsilon_p^{\text{ob}}) \propto \frac{L_{\text{iso}}}{E_{\text{peak}}^{\text{ob}} \Gamma^2 R} \times \begin{cases} \left(\frac{\epsilon_p^{\text{ob}}}{\epsilon_{pb}^{\text{ob}}} \right)^{-\beta-1}, & \epsilon_p^{\text{ob}} < \epsilon_{pb}^{\text{ob}} \\ \left(\frac{\epsilon_p^{\text{ob}}}{\epsilon_{pb}^{\text{ob}}} \right)^{-\alpha-1}, & \epsilon_p^{\text{ob}} \geq \epsilon_{pb}^{\text{ob}} \end{cases} \quad (9)$$

where Γ is the bulk Lorentz factor of GRB and R is the internal shock radius which relates with the bulk Lorentz factor and variability time δt through $R = 2\Gamma^2 c \delta t$. The break energy $\epsilon_{pb}^{\text{ob}}$ in the proton spectrum is caused by the break in the photon spectrum. Correspondingly, a break occurs in the neutrino spectrum at energy

$$\epsilon_{\nu b}^{\text{ob}} = 7.5 \times 10^{14} (1+z)^{-2} \Gamma_{2.5}^2 E_{\text{peak, MeV}}^{\text{ob}, -1} \text{eV}. \quad (10)$$

Additionally, there is another break in the neutrino spectrum caused by the synchrotron cooling of charged pions in the magnetic field of the dissipative fireball, which can be written as

$$\epsilon_{\nu c}^{\text{ob}} = 3.3 \times 10^{17} (1+z)^{-1} L^{-1/2} \Gamma_{2.5}^2 R_{14} \text{eV}. \quad (11)$$

The final neutrino spectrum (single flavor) of a GRB is approximately a three-section power law with two breaks at $\epsilon_{\nu b}^{\text{ob}}$ and $\epsilon_{\nu c}^{\text{ob}}$ respectively, i.e.,

$$\begin{aligned} (\epsilon_\nu^{\text{ob}})^2 \frac{dn_\nu}{d\epsilon_\nu^{\text{ob}}} &\simeq \frac{1}{8} \frac{\eta_p F_{\gamma, \text{bol}}}{\ln(\epsilon_{p, \text{max}}/\epsilon_{p, \text{min}})} f_{p\gamma}(\epsilon_\nu^{\text{ob}}) \\ &\times \begin{cases} (\epsilon_\nu^{\text{ob}})^{-\beta-1}, & \epsilon_\nu^{\text{ob}} < \epsilon_{\nu b}^{\text{ob}} \\ (\epsilon_\nu^{\text{ob}})^{-\alpha-1}, & \epsilon_{\nu b}^{\text{ob}} < \epsilon_\nu^{\text{ob}} < \epsilon_{\nu c}^{\text{ob}} \\ (\epsilon_\nu^{\text{ob}})^{-\alpha-3}, & \epsilon_{\nu c}^{\text{ob}} < \epsilon_\nu^{\text{ob}}. \end{cases} \end{aligned} \quad (12)$$

where η_p is the ratio between the energy in the accelerated protons and the radiation energy, $\epsilon_{p,\max}$ and $\epsilon_{p,\min}$ are respectively the maximum and minimum energy of accelerated protons, and $F_{\gamma,\text{bol}}$ is the bolometric (1 keV–10 MeV) gamma-ray fluence of the GRB. The factor 1/8 comes from the fact that half of the produced pions are charged pions and each neutrino takes about 1/4 of the pion’s energy.

3.2. Numerical results

In our numerical calculation, besides the Δ resonance channel, we also consider the contribution from the direct pion channel and the multi pion channel. The cross-section for photopion production is taken from Mücke et al. (2000) and the branching ratio of each channel is approximated as the same in H12. Muon cooling, pion cooling and neutrino oscillation effects are also included in the calculation. We calculate the GRB neutrino flux within the standard internal shock model, i.e., we use $R = 2\Gamma^2 c\delta t$, similar to the treatment by the IceCube Collaboration (Abbasi et al. 2010, 2011, 2012). We consider two cases of the choice of the bulk Lorentz factor Γ , one is the relation $\Gamma = 29.8E_{\text{iso},52}^{0.51}$ that is obtained by Ghirlanda et al. (2012), and another is the benchmark choice, i.e. $\Gamma = 10^{2.5}$ for all GRBs. As in H12, we fix $\delta t^{\text{ob}} = \delta t(1+z)$ at 0.01s. We assume the accelerated proton spectrum to be a power law with an index of -2 . The baryon ratio is taken to be $\eta_p = 10$.

We calculate the neutrino fluence from each GRB in the generated sample and the aggregated neutrino fluence from all the triggered GRBs in the sample is shown in Fig.3. To compare with the IceCube limit from the combined analysis of IC40 and IC59 for 215 GRBs, we have multiplied the aggregated fluence by a factor of $215/N_{\text{tri}}$, where $N_{\text{tri}} = 250$ is the number of triggered GRBs in our sample. The aggregated neutrino fluence peaks around 1 PeV and reach a level of $\sim 0.1\text{GeVcm}^{-2}$ for both choices of Γ . For comparison, we also show the fluence limit of IC40+59 in Fig.3 (dashed lines). The 90% upper limit on the fluence is obtained by requiring that the upgoing muon neutrino event number⁶ observed by IC40+59 should be smaller than $N_{\text{limit}} = 1.9$. The non-detection of neutrinos by IC40+59 implies $\eta_p \lesssim 20$. We note that the aggregated neutrino fluence of 215 GRBs in our former work H12 (see Fig. 2 in H12) is a factor of two lower and peaks at higher energy. The difference is due to that, in that work the luminosity and bulk Lorentz factor of all the GRBs without measured redshift are fixed as 10^{52}ergs^{-1} and $10^{2.5}$ respectively.

The diffuse neutrino flux can be obtained by multiplying the aggregated neutrino fluence of the all-sky GRBs occurred in one year by a factor of $1/4\pi\text{yr} \simeq 2.5 \times 10^{-9}\text{s}^{-1}\text{sr}^{-1}$. Fig. 4 presents the diffuse neutrino flux from all GRBs in our generated sample (solid lines), which consists of

⁶The upgoing muon neutrino number is obtained by summing up the contribution from every individual GRBs in the energy range of 0.1-3 PeV. For these upgoing neutrinos, we take $90^\circ - 180^\circ$ angle-averaged effective area for IC40 and IC59 in the calculation. The ratio of the number of GRBs calculated with the effective area of IC40 and IC59 is set to 117:98, in alignment with the realistic number ratio of GRBs that occurred during IC40 and IC59 operation period.

the flux contributed by the triggered GRBs (dashed line) and the flux contributed by untriggered GRBs (dash-dotted line). The top panel corresponds to the case that assumes $\Gamma = 29.8E_{\text{iso},52}^{0.51}$ (Ghirlanda et al. 2012) and the bottom to the case of $\Gamma = 10^{2.5}$. In both cases, the total flux around PeV energy are $\sim 10^{-9}\text{GeVcm}^{-2}\text{s}^{-1}\text{sr}^{-1}$. The flux produced by the untriggered GRBs is about a factor of two higher than that of the triggered ones.

In Fig. 5, we show the contribution to the diffuse neutrino flux by untriggered GRBs with different luminosity separately. As can be seen, GRBs in the intermediate luminosity range ($10^{51} - 10^{53}\text{ergs}^{-1}$) contribute the largest fraction of the diffuse neutrino flux in both cases of the choice of the bulk Lorentz factor. These GRBs do not trigger the detectors either due to occurring at relatively high redshifts, and/or due to having high spectral peaks (e.g., $E_{\text{peak}}^{\text{ob}} \gg 300\text{KeV}$). Besides, the occulted bright GRBs also contribute a significant fraction to the total neutrino flux.

3.3. Comparison with two PeV neutrinos

The IceCube Collaboration recently reported the detection of two cascade neutrinos in the range 1–10 PeV (Ishihara 2012), which are likely to be electron (or anti-electron) neutrinos. Several scenarios have been proposed to explain the origin of these two neutrinos (Barger et al. 2012; Baerwald et al. 2012; Bhattacharya et al. 2012; Roulet et al. 2012; Cholis & Hooper 2012). Since the energies of the reported two neutrinos are close to the peak energy of the typical GRB neutrino spectrum, we here study the possibility that they originate from diffuse GRB neutrinos. In studying the possible GRB origin, one must assure that the stacked neutrino flux of those 215 triggered GRBs observed by IceCube do not exceed the IC40+59 limit. The expected number of diffuse neutrinos from GRBs in the energy range 1–10PeV can be obtained by

$$N_{\text{diff}} = \int_{1\text{PeV}}^{10\text{PeV}} S(\epsilon_{\nu_e}) \left(\frac{dn_{\nu_e}}{d\epsilon_{\nu_e}} \right)_{\text{diff}} d\epsilon_{\nu_e}, \quad (13)$$

where $\left(\frac{dn_{\nu_e}}{d\epsilon_{\nu_e}} \right)_{\text{diff}}$ is the number spectrum of diffuse electron neutrinos (in unit of $\text{cm}^{-2}\text{s}^{-1}\text{sr}^{-1}\text{eV}^{-1}$) and $S(\epsilon_{\nu_e})$ is the IceCube exposure of electron neutrinos at ultra-high energies in 2 years (2010–2012) (Ishihara 2012), which includes the contribution by the Glashow resonance. Notably, since the analysis approach for diffuse cascade neutrinos is different from that for upgoing neutrinos from triggered GRBs, the IceCube effective area is significantly different. Based on the total diffuse neutrino flux we obtained above, we get $N_{\text{diff}} \approx 0.1$ for the case of $\Gamma = 29.8E_{\text{iso},52}^{0.51}$ and $N_{\text{diff}} \approx 0.2$ for the case of $\Gamma = 10^{2.5}$ ($\eta_p = 10$ is assumed). Since the non-detection of GRBs by IC40+59 implies $\eta_p < 20$ (see §3.2), we have $N_{\text{diff}} < 0.2$ or 0.4 respectively, which is insufficient to account for the reported two neutrinos. There is still a small possibility that these two neutrinos arise from, for instance, some very strong GRBs that happen to be occulted by the Earth and hence do not trigger the detectors. In addition, strong statistical fluctuation can also possibly lead to detection of one or two events.

3.4. Effect of variation in luminosity function and redshift distribution

There is significant variation in the luminosity function $\phi(L)$ and the rate distribution with redshift $\rho(z)$ in the literature (e.g. Firmani et al. 2004, G07, L07, W10, Zitouni et al. 2008; Cao et al. 2011). The variation may be caused by different approaches in obtaining the luminosity function and different spectral properties as well as trigger thresholds being used in the calculation.

Under the requirement that the total neutrino fluence from the triggered GRBs do not exceed the upper limit placed by IceCube, the possibility that GRBs are responsible for the two events increases if the fraction of neutrino flux from the untriggered GRBs increases. This requires more dim and/or distant GRBs to take place. Therefore, luminosity functions with steep slopes or rate distribution with higher rate at high redshift are favorable for producing more dim, untriggered GRBs. As the slopes in the luminosity function of L07 below and above the break luminosity L_b are shallower than that in W10, adopting this luminosity function will lead to a smaller fraction of untriggered GRBs. However, the rate redshift distribution used in L07 suggests higher rate of GRBs at high redshift, which, on the contrary, will lead to a higher fraction of untriggered GRBs. We estimate that the neutrino flux produced by untriggered GRBs is about 90% of that of triggered GRBs for the luminosity function and rate distribution in L07. For the luminosity function and rate distribution in G07, this factor increases to 2.5 because of the steep slope in the luminosity function of G07 and higher GRB rate at high redshift. Even considering the variation in the luminosity function and rate distribution in the literature, the diffuse neutrino flux from GRBs may be still insufficient to account for the two neutrinos.

4. Discussions

Other possible sources of dim, untriggered GRBs are low-luminosity GRBs (LLGRBs) and Population III (Pop III) GRBs. LLGRBs are GRBs with luminosity $\lesssim 10^{49} \text{ergs}^{-1}$, which constitute a distinct population from the normal GRBs (e.g. Soderberg et al. 2006; Liang et al. 2007; Dai 2009; Virgili et al. 2009). Although only several cases are observed within $\sim 200 \text{Mpc}$ so far, which is mainly due to their low luminosity, the intrinsic local event rate of LLGRBs is suggested to be about two orders of magnitude higher than that of the normal GRBs (e.g. Liang et al. 2007; Dai 2009; Virgili et al. 2009). Thus, the large local population could compensate for the low energy in LLGRBs, and lead to a significant amount of neutrino flux (e.g. Murase et al. 2006; Gupta & Zhang 2007; Murase et al. 2008; Liu et al. 2011). In Liu et al. (2011), we calculated the diffuse neutrino flux from LLGRBs for different LLGRB luminosity functions and found that the flux can reach a level of $\sim 10^{-9} \text{GeVcm}^{-2}\text{s}^{-1}\text{sr}^{-1}$ or higher around PeV energies, depending on the parameters of LLGRBs that are used, such as the choice of Γ . We also found that most LLGRBs are untriggered and the energy budget of gamma rays in untriggered LLGRBs can be several times larger than that in the triggered ones. Thus more than 0.2–0.4 electron neutrinos in the range 1–10 PeV could come from LLGRBs in principle. However, since the origin of LLGRBs are not clear (e.g. Wang et al.

2007) and the properties of LLGRBs have large uncertainties, we should be cautious about this estimate.

Pop III GRBs are thought to arise from the death of the first stars that locate at high redshift ($z \gtrsim 10$). It is suggested that their luminosity is typically a few times $10^{52} \text{ ergs}^{-1}$ and their duration is $\gtrsim 10^4 \text{ s}$ (Mészáros & Rees 2010; Komissarov & Barkov 2010; Suwa & Ioka 2011), so they may release energy up to 10^{56-57} erg in one burst. At such large distances, their gamma-ray flux is below $\sim 10^{-8} \text{ erg cm}^{-2} \text{ s}^{-1}$, so they may not be able to trigger current GRB detectors. Thus, if Pop III GRBs can produce high energy neutrinos, these neutrinos will contribute to the diffuse background. It has been shown by Iocco et al. (2008); Gao et al. (2011) that the neutrino flux in 1-10 PeV range can reach $\sim 10^{-9} \text{ GeV cm}^{-2} \text{ s}^{-1} \text{ sr}^{-1}$, or even $\sim 10^{-8} \text{ GeV cm}^{-2} \text{ s}^{-1} \text{ sr}^{-1}$ when some preferred parameters are used, e.g., with large progenitor mass and/or high interstellar medium density. However, since the flux peaks at $\sim 10^{17} \text{ eV}$, one would expect even stronger flux at $\sim 10^{17} \text{ eV}$, which is inconsistent with the non-detection by IceCube at such energies. Moreover, the rate of Pop III GRBs is quite uncertain. The Pop III GRB rate adopted in Gao et al. (2011) is from Bromm & Loeb (2006), which obtains a much higher rate than that in de Souza et al. (2011) and Campisi et al. (2011). So whether Pop III GRBs are responsible for the two neutrinos remains to be studied.

Finally we note that we only consider the neutrino emission under the standard internal shock model. For other models for the GRB prompt emission, such as the photosphere emission models (e.g. Rees & Mészáros 2005) or magnetically reconnection models (e.g. Zhang & Yan 2011), the efficiency for producing neutrinos $f_{p\gamma}$ is different (e.g. Wang & Dai 2009; Zhang & Kumar 2012), due to different dissipation radii R involved. However, the ratio between the flux from triggered GRBs and that from untriggered GRBs is not expected to change. Therefore, the diffuse neutrino flux can not be readily increased under the constraint that no neutrinos are detected from triggered GRBs.

5. Conclusions

In this paper, we studied the diffuse neutrino emission from GRBs in light of the recent report that two PeV cascade events are detected by IceCube. We first generate a GRB sample that reproduces the realistic properties of the observed GRBs by Fermi/GBM. An accompanying sample of untriggered GRBs is generated simultaneously. Then we calculated the neutrino flux from the triggered and the untriggered GRBs in the sample within the standard internal shock scenario. The advantage of this approach is that the spectral properties (i.e. the spectral peak and indices) of every individual GRBs can be taken into account properly in the calculation. We found that the neutrino flux from the untriggered GRBs is about a factor of two larger than that of the triggered GRBs. Under the constraint of the non-detection of any upgoing muon neutrinos from 215 triggered GRBs in the IC40+59 combined analysis, the total diffuse neutrinos flux (single flavor) can reach a level of $\sim 10^{-9} \text{ GeV cm}^{-2} \text{ s}^{-1} \text{ sr}^{-1}$ at most. Such a flux can only give rise to $\lesssim 0.2 - 0.4$ cascade

neutrino events in 1–10 PeV for IceCube 2-years exposure. Low-luminosity GRBs and/or Pop III GRBs can also contribute to the diffuse neutrino flux, but large uncertainties in their properties prevents us from drawing a firm conclusion.

We thank Kohta Murase, Jun Kakuwa, Aya Ishihara, Shigeru Yoshida and Ilias Cholis for useful discussions. This work is supported by the 973 program under grant 2009CB824800, the NSFC under grants 10973008, 11273016 and 11033002, the Excellent Youth Foundation of Jiangsu Province and the Fok Ying Tung Education Foundation.

REFERENCES

- Abbasi, R., Abdou, Y., Abu-Zayyad, T., et al. 2010, *ApJ*, 710, 346
- Abbasi, R., Abdou, Y., Abu-Zayyad, T., et al. 2011a, *Physical Review Letters*, 106, 141101
- Abbasi, R., Abdou, Y., Abu-Zayyad, T., et al. 2011b, *Phys. Rev. D*, 84, 082001
- Abbasi, R., Abdou, Y., Abu-Zayyad, T., et al. 2011, *Phys. Rev. D*, 83, 092003
- Abbasi, R., Abdou, Y., Abu-Zayyad, T., et al. 2012, *Nature*, 484, 351
- Amati, L., Frontera, F., Tavani, M., et al. 2002, *A&A*, 390, 81
- Baerwald, P., Hümmer, S., & Winter, W. 2012a, *Astroparticle Physics*, 35, 508
- Baerwald, P., Bustamante, M., & Winter, W. 2012b, *JCAP*, 10, 20
- Band, D., Matteson, J., Ford, L., et al. 1993, *ApJ*, 413, 281
- Barger, V., Learned, J., & Pakvasa, S. 2012, *arXiv:1207.4571*
- Bhattacharya, A., Gandhi, R., Rodejohann, W., & Watanabe, A. 2012, *arXiv:1209.2422*
- Bromm, V., & Loeb, A. 2006, *ApJ*, 642, 382
- Butler, N. R., Bloom, J. S., & Poznanski, D. 2010, *ApJ*, 711, 495
- Campisi, M. A., Maio, U., Salvaterra, R., & Ciardi, B. 2011, *MNRAS*, 416, 2760
- Cao, X.-F., Yu, Y.-W., Cheng, K. S., & Zheng, X.-P. 2011, *MNRAS*, 416, 2174
- Cholis, L. & Hooper, D., 2012, *arXiv:1211.1974*
- Dai, X. 2009, *ApJ*, 697, L68
- Dermer, C. D. 2002, *ApJ*, 574, 65

- Dermer, C. D., & Atoyan, A. 2006, *New Journal of Physics*, 8, 122
- de Souza, R. S., Yoshida, N., & Ioka, K. 2011, *A&A*, 533, A32
- Firmani, C., Avila-Reese, V., Ghisellini, G., & Tutukov, A. V. 2004, *ApJ*, 611, 1033
- Gao, S., Toma, K., & Mészáros, P. 2011, *Phys. Rev. D*, 83, 103004
- Ghirlanda, G., Nava, L., Ghisellini, G., et al. 2012, *MNRAS*, 420, 483
- Guetta, D., Hooper, D., Alvarez-Muniz, J., Halzen, F., & Reuveni, E. 2004, *Astroparticle Physics*, 20, 429
- Guetta, D., & Piran, T. 2007, *JCAP*, 7, 3
- Gupta, N., & Zhang, B. 2007, *Astroparticle Physics*, 27, 386
- He, H.-N., Liu, R.-Y., Wang, X.-Y., et al. 2012, *ApJ*, 752, 29
- Hümmer, S., Baerwald, P., & Winter, W. 2012, *Physical Review Letters*, 108, 231101
- Iocco, F., Murase, K., Nagataki, S., & Serpico, P. D. 2008, *ApJ*, 675, 937
- Ishihara, A., A plenary Talk at the Neutrino 2012 Workshop, June 8th, 2012, Kyoto, Japan.
- Kakuwa, J., Murase, K., Toma, K., et al. 2012, *MNRAS*, 425, 514
- Kaneko, Y., Preece, R. D., Briggs, M. S., et al. 2006, *ApJS*, 166, 298
- Karle, A., & for the IceCube Collaboration 2010, *arXiv:1003.5715*
- Komissarov, S. S., & Barkov, M. V. 2010, *MNRAS*, 402, L25
- Li, Z. 2012, *Phys. Rev. D*, 85, 027301
- Liang, E., Zhang, B., Virgili, F., & Dai, Z. G. 2007, *ApJ*, 662, 1111
- Liang, E.-W., Yi, S.-X., Zhang, J., et al. 2010, *ApJ*, 725, 2209
- Liu, R.-Y., Wang, X.-Y., & Dai, Z.-G. 2011, *MNRAS*, 418, 1382
- Lü, J., Zou, Y.-C., Lei, W.-H., et al. 2012, *ApJ*, 751, 49
- Meegan, C., Lichti, G., Bhat, P. N., et al. 2009, *ApJ*, 702, 791
- Mészáros, P., & Rees, M. J. 2010, *ApJ*, 715, 967
- Mücke, A., Engel, R., Rachen, J. P., Protheroe, R. J., & Stanev, T. 2000, *Computer Physics Communications*, 124, 290

- Murase, K., & Nagataki, S. 2006, Phys. Rev. D, 73, 063002
- Murase, K., Ioka, K., Nagataki, S., & Nakamura, T. 2006, ApJ, 651, L5
- Murase, K., Ioka, K., Nagataki, S., & Nakamura, T. 2008, Phys. Rev. D, 78, 023005
- Porciani, C., & Madau, P. 2001, ApJ, 548, 522
- Rees, M. J. & Mészáros, P. 2005, ApJ, 628, 847
- Roulet, E., Sigl, G., van Vliet, A., & Mollerach, S. 2012, arXiv:1209.4033
- Rowan-Robinson, M. 1999, Ap&SS, 266, 291
- Soderberg, A. M. 2006, Nature, 422, 1014
- Suwa, Y., & Ioka, K. 2011, ApJ, 726, 107
- The Fermi Large Area Telescope Team, Ackermann, M., Ajello, M., et al. 2012, ApJ, 754, 121
- Vietri, M. 1995, ApJ, 453, 883
- Virgili, F. J., Liang, E.-W., & Zhang, B. 2009, MNRAS, 392, 91
- Wanderman, D., & Piran, T. 2010, MNRAS, 406, 1944
- Wang, X. Y., Li, Z., Waxman, E. & Mészáros, P., 2007, ApJ,
- Wang, X.-Y., Razzaque, S., & Mészáros, P. 2008, ApJ, 677, 432
- Wang, X.-Y., & Dai, Z. G., 2009, ApJ, 691, L67
- Waxman, E. 1995, Physical Review Letters, 75, 386
- Waxman, E., & Bahcall, J. 1997, Physical Review Letters, 78, 2292
- Yonetoku, D., Murakami, T., Nakamura, T., et al. 2004, ApJ, 609, 935
- Zhang, B., & Yan, H. R., 2011, ApJ, 726, 90
- Zhang, B., & Kumar, P. 2012, arXiv:1210.0647
- Zitouni, H., Daigne, F., Mochkovich, R., & Zerguini, T. H. 2008, MNRAS, 386, 1597

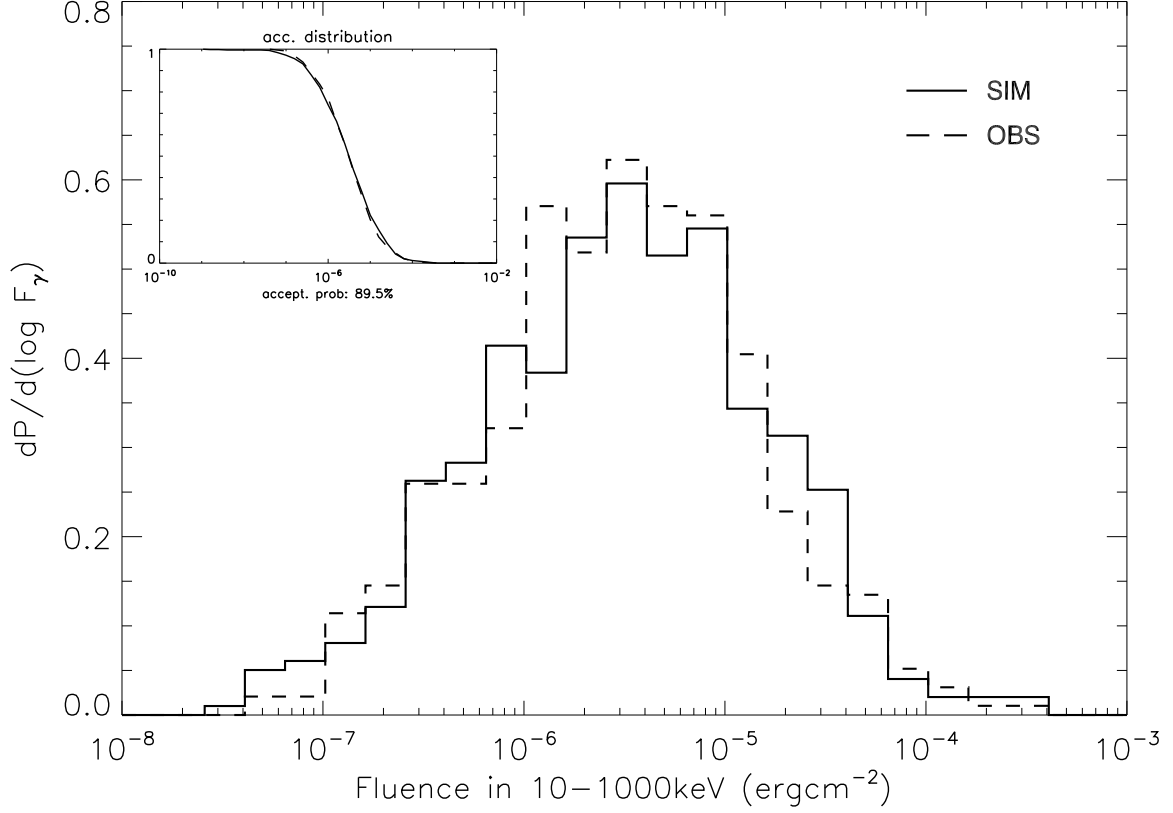


Fig. 1.— Comparison of the fluence (10-1000 keV) distribution of GRBs in the generated sample and in the observed sample by Fermi/GBM. The solid line and dashed line represent the triggered GRBs in our generated sample and the observed sample respectively. The K-S test gives a probability of 89.5% for the agreement the two distributions. The inset figure shows the distributions of accumulated fluence of these two samples.

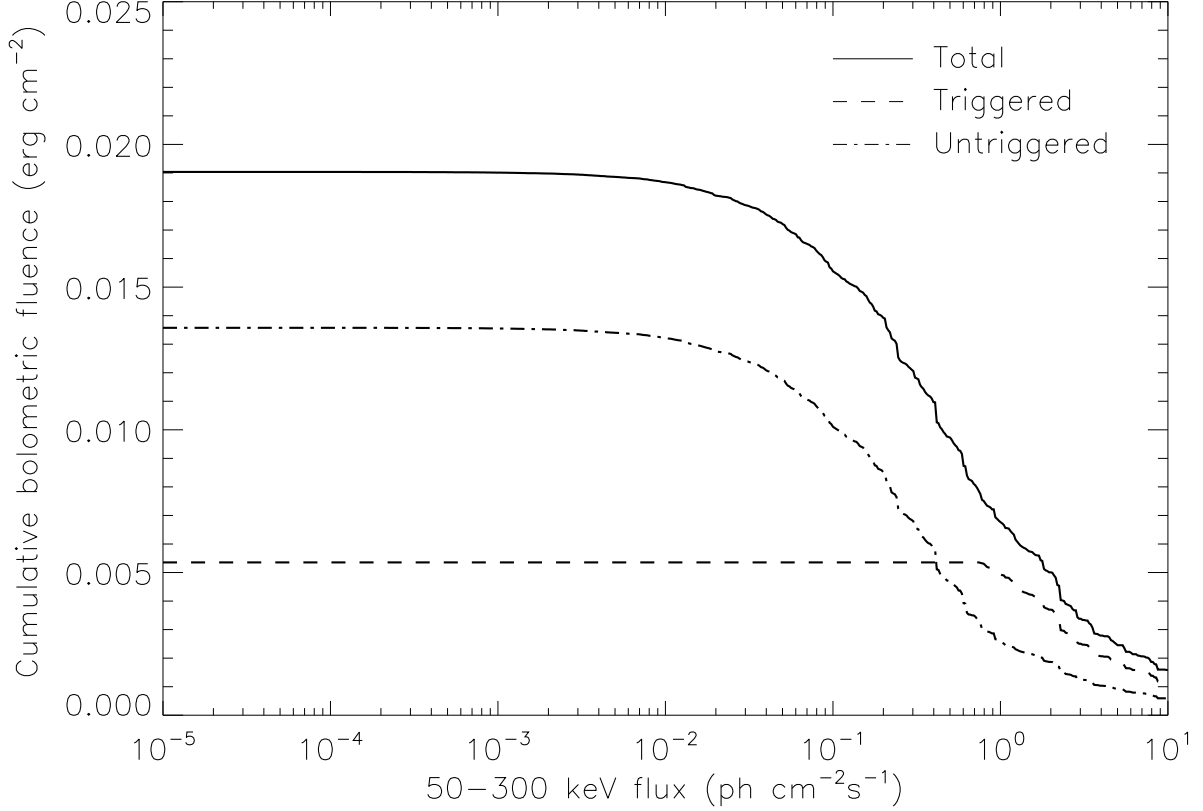


Fig. 2.— Cumulative bolometric fluence (1-10000 keV) as a function of the flux (50-300KeV) of GRBs in the generated sample. The triggered GRBs, untriggered GRBs and the total are represented by the dashed line, dot-dashed line and solid line respectively. Since about 35% GRBs with flux above the trigger threshold are ascribed to untriggered GRBs due to occultation by the Earth and the South Atlantic Anomaly passages, the cumulative fluence of untriggered GRBs is non-zero below the Fermi/GBM trigger threshold $0.74 \text{ ph cm}^{-2} \text{ s}^{-1}$.

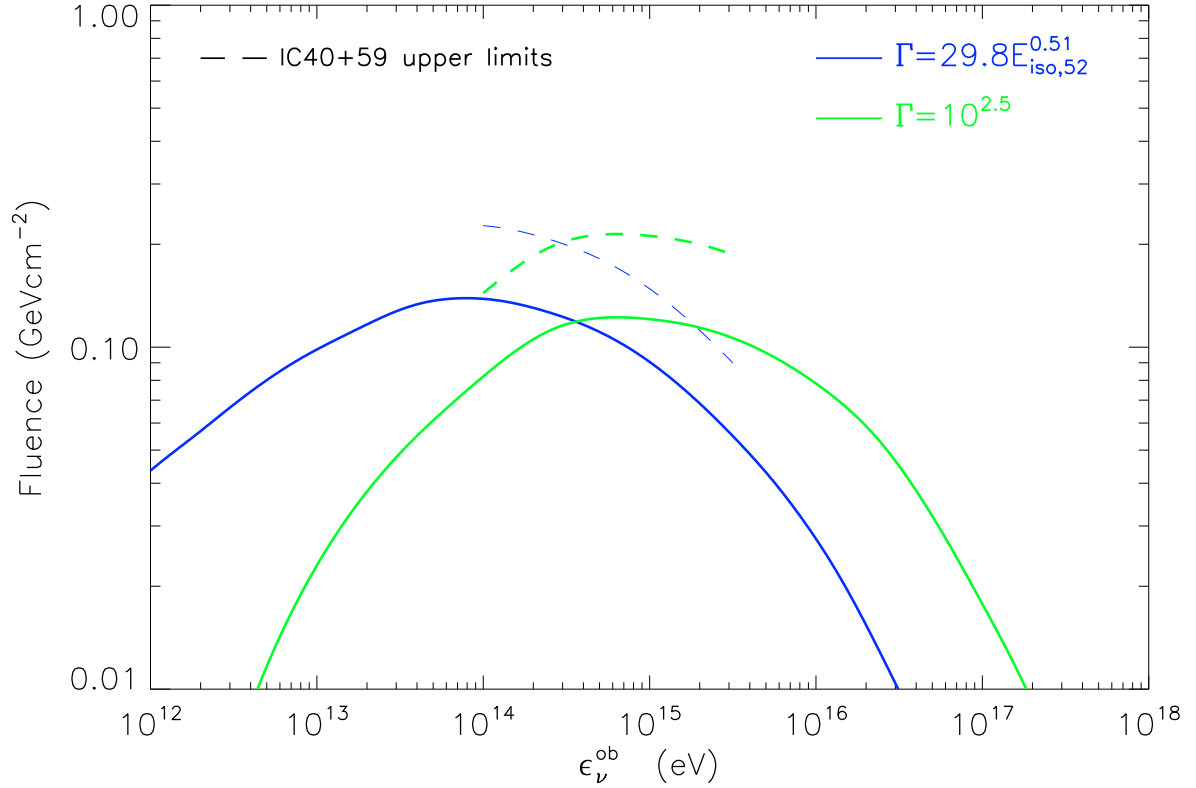


Fig. 3.— The aggregated neutrino fluence spectrum (single flavor) from triggered GRBs in our generated sample. The blue and green solid lines represent the fluence obtained assuming $\Gamma = 29.8 E_{\text{iso},52}^{0.51}$ (Ghirlanda et al. 2012) and the benchmark value $\Gamma = 10^{2.5}$ respectively. The corresponding dashed lines represent the 90% upper limits from IC40+59. In the calculation, we assumed that the proton spectrum is a power law with index of -2 and $\eta_p = 10$.

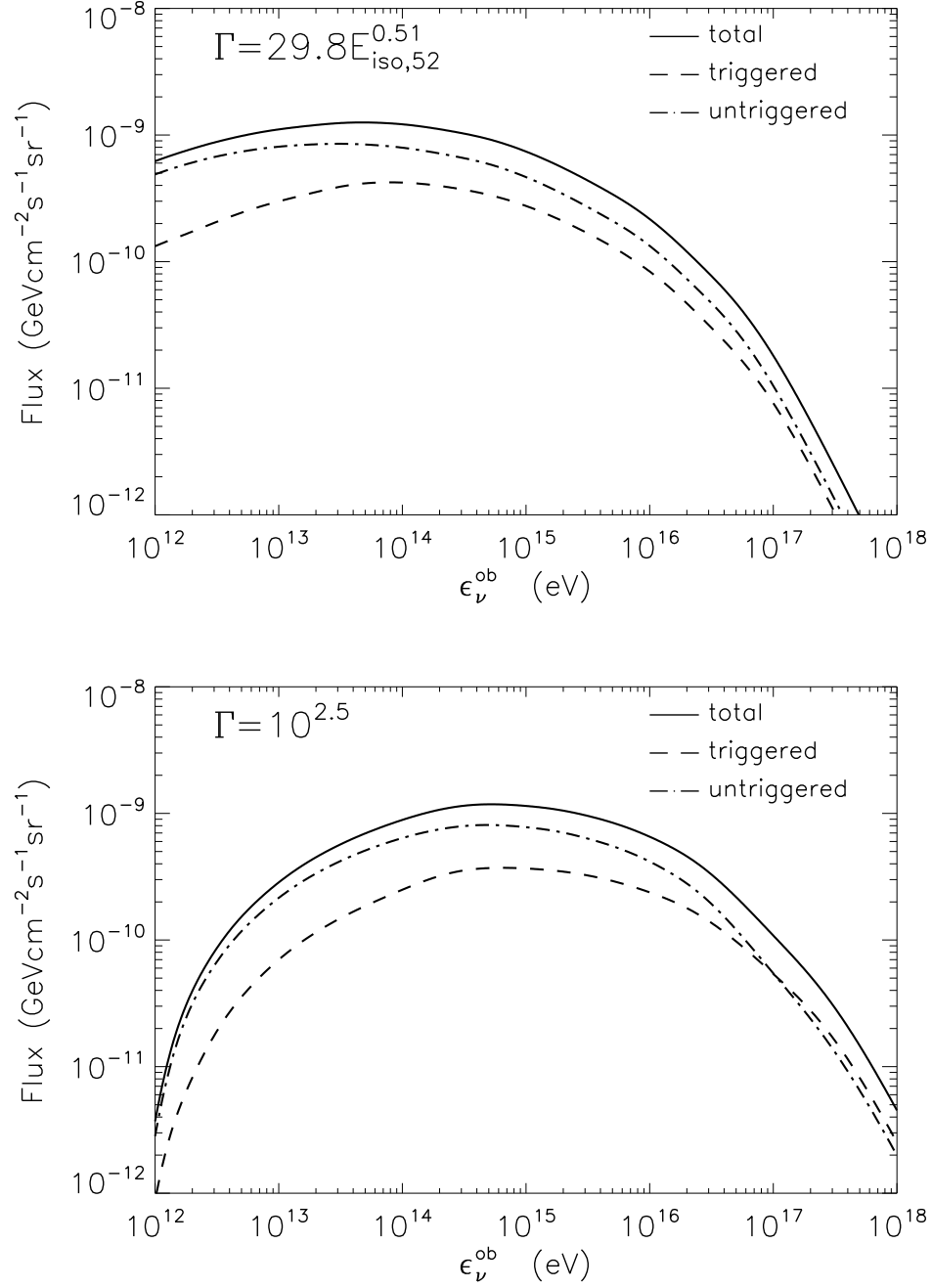


Fig. 4.— The diffuse neutrino flux from GRBs in our generated sample. The dashed line and the dash-dotted line represent the contribution by the triggered GRBs and untriggered GRBs respectively, and the solid line represents the total flux. In the top panel $\Gamma = 29.8 E_{\text{iso},52}^{0.51}$ is used, while in the bottom panel Γ is fixed at $10^{2.5}$. We assumed that the proton spectrum is a power law with index of -2 and $\eta_p = 10$.

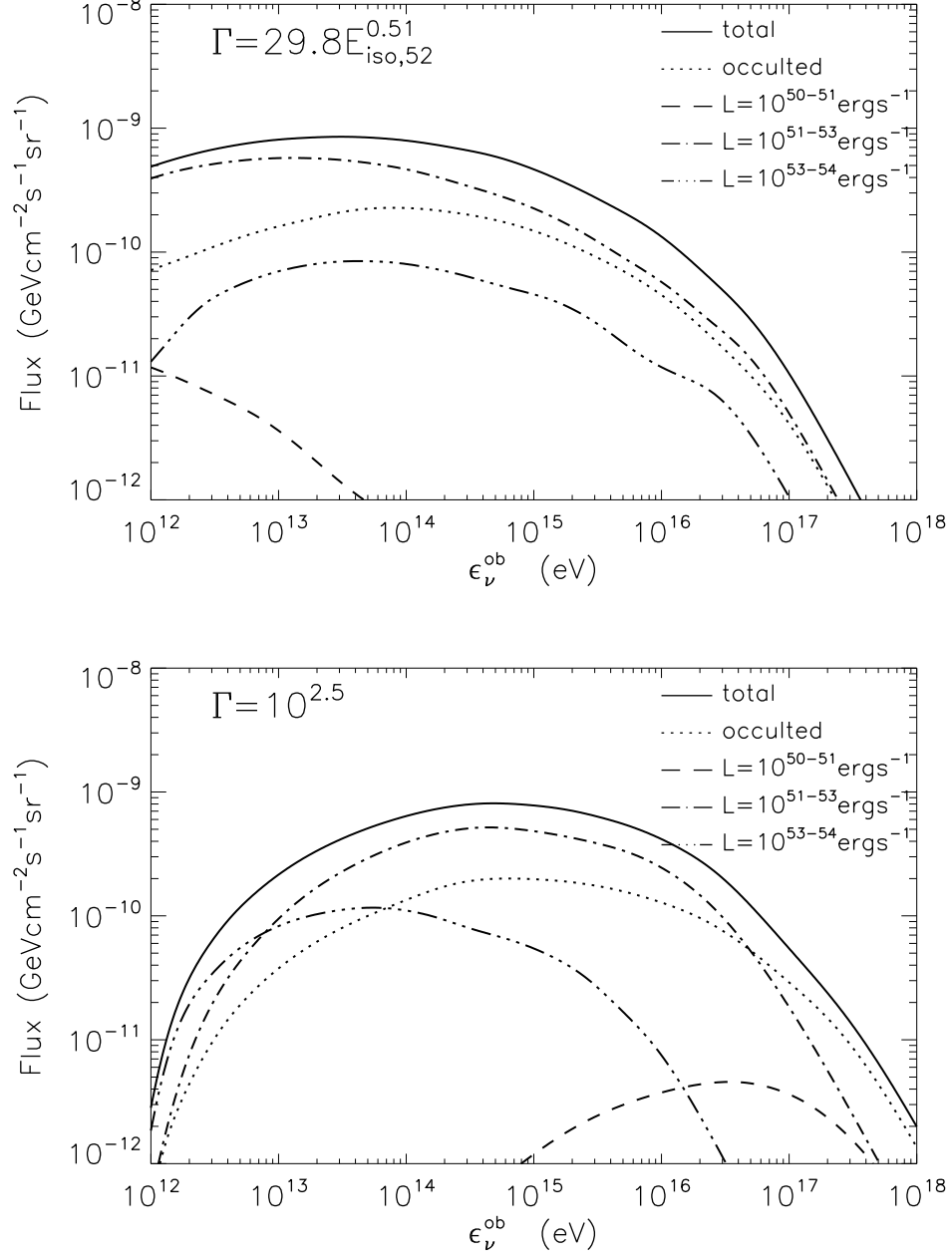


Fig. 5.— Contribution to the diffuse neutrino flux by untriggered GRBs with different luminosity. The dotted lines represent the contribution by the occulted bright GRBs. The dashed lines, dash-dotted lines and the long dash-dotted lines represent the contributions from GRBs in different luminosity ranges respectively (not including those occulted GRBs). The solid lines represent the sum of the four components.).